

THE DESIGN AND SIMULATION OF MPPT CONTROLLED DC-DC BOOST CONVERTER AS SOLAR BATTERY CHARGER

Bassam Al-HANAHI

Department of Electrical Engineering, Yildiz Technical University, Istanbul, Turkey.
Email: alhanahi.bassam@gmail.com

Burak AKIN

Department of Electrical Engineering, Yildiz Technical University, Istanbul, Turkey.
Email: bakin@yildiz.edu.tr

Abstract: *In this paper, the design of MPPT controlled DC-DC boost converter for PV charger application is presented. Duty cycle of the designed converter, which operates in 50 KHz, is controlled directly by Incremental conductance algorithm in order to track maximum power point of the PV panel that is changing in response of variation irradiance of sunny day. The designed converter is used as interface unit for matching 24V battery bank (20AH, 12V, C/5) with CANADIAN SOLAR CS5C-90 panel. The overall system is built and validated by using MATLAB SIMULINK. The simulation is performed under two cases of environmental conditions which are slow and fast changing conditions. In addition, the performance of simulated MPPT system is measured in term of tracking efficiency, conversion efficiency, and response time. The simulation results show that the proposed converter has averaged tracking efficiency of 98% and 97.55% and averaged conversion efficiency of 98.52% and 98.24% for slow and fast changing conditions respectively, and response time in the range of 70 ms, which is measured over the simulation time of 2.5s for both conditions. These results express the high performance and effective operation of designed converter, as compared with other systems in literature.*

Key words: Boost Converter, MPPT Algorithms, Solar Panel, Solar charger.

1. Introduction

Non-renewable energy sources have a limited supply, often releasing harmful gases, and their prices are increasing continuously. These have become the main driving forces to use renewable energy sources, such as solar, wind, biomass and hydropower energy. As compared to other sources, solar energy is more attractive since it is environmentally clean, abundantly available, cheap, and easily transferrable to other forms of energy. One practical application of solar energy is solar photovoltaic panels as a source of electricity. PV panels can be connected to grid systems as renewable power plant that provides power into system. In addition, the availability of energy storage system, such as batteries, enables PV panels to be used in stand-alone solar systems. Stand-alone systems are not part of the grid and are essential for regions that are remote from public grid. In these systems, batteries are used to either supply load when

PV panel has not enough energy because of low irradiance, or supply load continuously as in the case of some application such as electric vehicle and lighting systems. In both case of application, battery should be charged by PV system fully and safely as fast as possible for high performance and reliability of stand-alone [1].

However, power extracted from PV panel is restricted due to certain limitations. The first limitation is the low efficiency of PV panel in converting solar energy into electricity (10 to 16% efficiency for amorphous silicon solar cells). Secondly, because of highly nonlinearity of P-V and I-V characteristic curves of PV panel, there is only one operating point, which called maximum power point (MPP), at which PV panel provides maximum available power. In addition, this MPP point is not fixed and depends on environmental conditions such as temperature and insolation level. In consequence, the direct connection of the PV panel and load (or battery) reduces the power that could be supplied to load (or battery), if the operating point of load (or battery) and Maximum power point (MPP) of PV array are not in concurrence, which is the normal case of operation. Therefore, the performance of load (or battery) will be affected badly [2, 3].

In order to continuously obtain the maximum available power from the solar panels; thus improve the performance of supplied load (or battery), it is necessary to match the operating point of load (or battery) with MPP of PV panel. This matching can be done by inserting an interface unit between PV system and load. This unit is called a maximum power point tracking (MPPT). In this manner, the MPPT system continuously tracks the peak power condition by monitoring the output voltage and current of the solar panel and determines the optimum operating point of PV panel; thus increasing the efficiency of extracting power from the solar panels. MPPT system consists of two main components. Firstly, MPPT algorithms which determine the required operating point for maximum power

generation of PV panels. Secondly, DC-DC converters which perform the tracking action by controlling its duty cycle according to the determined operating point [4].

In this paper, the design and modelling of MPPT system is simulated by using SIMULINK. In this simulation, CANADIAN SOLAR CS5C-90 panel is used to charge 24V battery bank (12V 20AH C/5) through MPPT system. Generally, the simulated model of battery should involve all parameters that affect the performance of battery, such as charging current, charging voltage, state of charge, temperature of battery. However, in this simulation, because the operation of MPPT system in extracting maximum power is under consideration, battery is represented ideally by constant voltage. In this simulation, MPPT system model composes of boost converter model which its duty cycle is controlled directly by InC algorithm.

The proposed design MPPT system in this paper has superiority over many systems that have been proposed in literature. In [2], the design of MPPT system is similar to the one proposed in this system. In that study, InC algorithm is used to control boost converter. The conversion efficiency of that MPPT system is 92% which is compared with 98.52% obtained in this paper. Furthermore, the high conversion efficiency of proposed system in this paper has been approved in different environment conditions.

In [5], the two phase interleaved boost converter is used in the design of DC-DC converter which is controlled by InC algorithm. The topology is used in order to reduce the ripples in input voltage and current. However, this topology reduces the conversion efficiency and increases the cost of MPPT system due to the additional inductor. In this paper, the input capacitor reduces the ripples of input voltage and current with lower cost and higher efficiency of designed MPPT system

In another study [6], the Interleaved Fly-back converter is used in the design of DC-DC converter. This study is based on comparing the performance of three different algorithms with the selected topology of converter. The maximum tracking efficiency in this study is 98.26% which is achieved by InC algorithm. This efficiency is compared with that achieved in this paper. However, the implementation of MPPT system in [6] is complex and costly as compared to the system of this paper.

In order to express the superiority of proposed MPPT system in this paper, the high performance of proposed system, which is measured in term of tracking efficiency, conversion efficiency, and response time of MPPT system, is analyzed in more details under different conditional environment.

2. PV Solar Charger Characteristics

2.1 PV Panel Model

PV panels comprise of many solar cells, which are connected part by part in integrated series and parallel, as building blocks. A solar cell converts sun energy into electricity by means of the photoelectric action that could be found in specified types of semiconductor materials such as silicon i.e. generates electric voltage and current on exposure to light. The ideal PV cell is modelled as single diode circuit as shown in Fig. 1. This circuit contains of a current source, a diode in parallel with source, series resistors R_s , and parallel R_{sh} to represent dissipation of PV cell [7].

The relation between voltage and current of PV panel can be described, mathematically, as in (1).

$$I = I_{PV} - I_o [\exp((V + R_s I)/kT) - 1] - (V + R_s I)/R_p \quad (1)$$

Where, I is the PV cell current (A). I_{PV} is the PV cell photocurrent (A). I_o is the diode saturation current. T is the cell temperature (K). R_s and R_p are the series and shunt resistance of PV cell (ohms) and V is the output voltage of PV cell (V) [8]

Equation (1) of the ideal PV cell does not define the I-V characteristic of a practical PV array. Practical arrays are manufactured by using several connected PV cells and the determination of the characteristics is done at the terminals of the PV array.

If the array is composed of N_p parallel connections of cells the PV and saturation currents may be expressed as in (2) and (3).

$$I_{PV} = I_{PV,cell} * N_p \quad (2)$$

$$I_o = I_{o,cell} * N_p \quad (3)$$

Where R_s is the equivalent series resistance of the array and R_p is the equivalent parallel resistance [8].

Terminal characteristics of PV panel are represented as P-V and I-V curves which are generally supplied by manufacturer. These curves have highly nonlinear characteristics and depend on environmental conditions where PV panel is located.

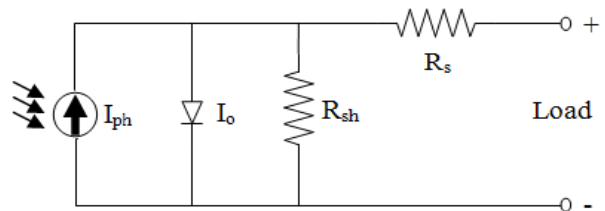


Fig. 1. Single diode circuit modelling of ideal PV cell

2.2 Boost Converter Model

Boost topology is chosen for DC-DC converter since it is capable of transferring maximum energy from PV panel to load irrespective of different irradiation of sun through the day. The topology of converter is shown in Fig. 2. It consists of dc source V_S , inductor L , power switch S , diode D , output capacitor C , and output load R . When the switch S is in the on state, the current in the inductor increases linearly and the diode D is off at that time. The load is supplied by the output capacitor. When the switch S is turned into off state, both the source and the energy stored in the inductor is transferred through the diode to the output load [9].

The converter waveforms in the CCM are presented in Fig. 3. As shown in the waveform for inductor voltage, in the first period the inductor is supplied with V_S and in the second period the $(V_S - V_O)$ voltage with reversed polarity is induced across the inductor to keep flowing of current in the same direction, where V_O is the output voltage [9].

According to Fig. 3, change of inductor current in both periods (ΔI_{LP} and ΔI_{LN}) could be written as in (4) and (5).

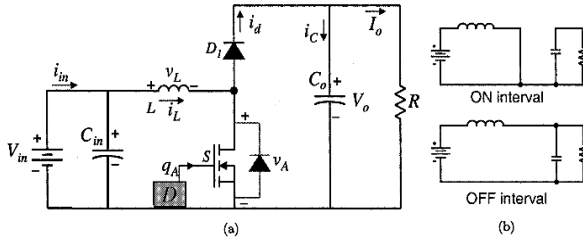


Fig. 2. Boost converter topology equivalent circuit

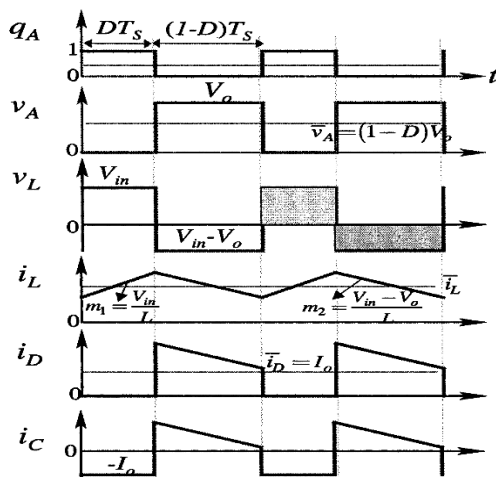


Fig. 3. Boost converter waveforms in the CCM

$$\Delta I_{LP} = (V_S/L)DT \quad (4)$$

$$\Delta I_{LN} = (V_O - V_S/L)(1 - D)T \quad (5)$$

In steady state operation, the positive and negative periods of inductor voltage waveform are equal and accordingly the rising and falling of inductor currents.

Equations (4) and (5) could be written as in (6).

$$V_S DT = (V_O - V_S)(1 - D)T \quad (6)$$

From (6), average output voltage could be obtained as in (7).

$$V_O = (1/(1 - D)) V_S \quad (7)$$

The output voltage of the converter could be controlled between $V_S < V_O < V_{\max}$, where V_{\max} is the maximum required output voltage [9].

2.3 Boost Converter Design Process

To design and size the components of boost converters, many factors should be considered such as, input voltage to converter, output voltage magnitude, DC-DC converter efficiency, output voltage ripple, input power, desired output power, input current, output current and duty cycle of PWM controller.

There are five components that should be chosen when boost converter is designed. These are power switching device, diode, inductor, output capacitor, and input capacitor. [9].

- Power switching device: The main switching device must withstand the maximum current and voltage stresses and also operate at the desired frequency [9].

- Diode: Diode must be characterized by capability of withstanding the required reversed off-state voltage stress as well as the maximum and average current. In addition, it must have low forward voltage drop, reduced reverse-recovery, and fast switching capability [10].

- Inductor: the design of boost inductor depends on the maximum required ripple current which is determined at minimum duty cycle and maximum input voltage. The value of boost inductor is determined for specific load as shown in (8), where F_s is the operating switching frequency.

$$L = (V_S * (V_O - V_S)) / (\Delta I_{LP} * F_s * V_O) \quad (8)$$

Regarding the current flowing in inductor, the boost converter can operate in continuous mode of operation (CCM) and discontinuous mode of operation (DCM). For CCM of operation, the minimum inductance required (L_{\min}) is calculated as can be shown in (9).

$$L_{MIN} = (V_S * (V_O - V_S)) / (2 * I_S * F_S * V_O) \quad (9)$$

Where I_S is the source current. When F_S is selected, there should be a trade-off between minimizing the size of the inductor and limiting the loss of the power switching device. Generally, high-frequency of F_S is imposed and it should be checked if the current ripple is correct by low frequency [10, 2].

- **Output capacitor:** Output capacitor must be designed carefully to perform two important functions. Firstly, it must limit the output voltage ripple as well as withstand the required ripple current stress. The second function, it must supply the required output current to the load when the diode is off state. The minimum value of the output capacitance that provides the specified voltage ripple (ΔV_O) is calculated as in (10). In addition, the required ESR that give the required voltage ripple could be determined as in (11) [10, 11].

$$C_{min} = (I_O * D) / (F_S * \Delta V_O) \quad (10)$$

$$ESR \leq \Delta V_O / ((I_S + (\Delta I_{LP}) / 2)) \quad (11)$$

- **Input capacitor:** The minimum value of input capacitor is necessary to regulate the input voltage due to the current requirement of power supply. This minimum value can be increased in case of noisy input [11].

3. Incremental Conductance Algorithm.

The InC algorithm is one of the most commonly used technique because its cost is low and implementation is easy. This algorithm depends on the fact that the derivative of conductance at MPP is equal to the negative instantaneous conductance. [12]

Figure 4 shows chart of InC algorithm. As can be shown, the operation of this algorithm is initialized by sensing the operating point of PV panel at successive (n) and (n+1) instants. Depending on these operating points, the incremental conductance is calculated as $(\Delta I / \Delta V)$ and compared to the instantaneous conductance (I / V). The process continues until the incremental conductance equals the negative instantaneous conductance $((\Delta I / \Delta V) = (-I / V))$. [12]

In practical, there is steady state oscillation of power around MPP. In this case, MPP of PV panel is detected when $((\Delta I / \Delta V) + (I / V))$ is within the tolerance band. [12]

This tolerance band can be controlled by step size of perturbation. The selection of step size is tradeoff between steady state oscillation and speed of performance of algorithm [12].

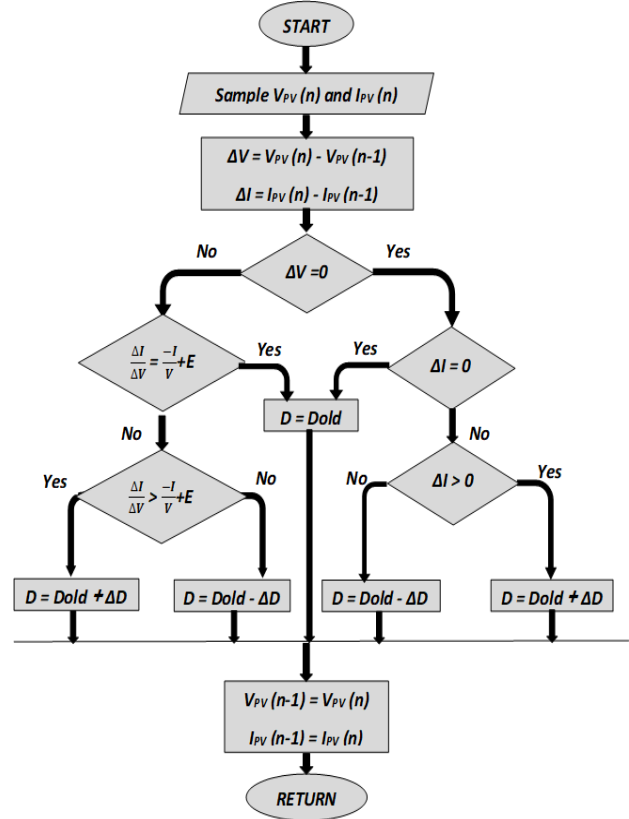


Fig. 4. MPPT InC algorithm chart

4. Simulated PV System Model

Figure 5 shows the simulated PV system which is constructed by Simulink in MATLAB. The simulated system consists of PV array, MPPT controller, DC-DC boost converter and the battery.

In this simulation, CANADIAN SOLAR CS5C-90 panel is used for simulating PV array. The specification parameters of the used PV panel are listed in Table 1. The maximum power of 90W is given Under Standard Test Conditions (STC) of irradiance of 1000 W/m², spectrum AM 1.5 and cell temperature of 25°C.

Figure (6) and (7) represents P-V and V-I curves of this panel for different irradiance levels. These curves represent maximum power that can be extracted from PV panel in different level of insolation.

In this simulation, the design of boost converter is performed according to the equations (7-11). According to the requirements of charging, the design specifications are listed in Table 2. As mention, five parameters should be determined when designing of boost converter. The Schottky diode and IGBT switch is chosen to withstand the maximum stress of current and voltage of system under operating frequency.

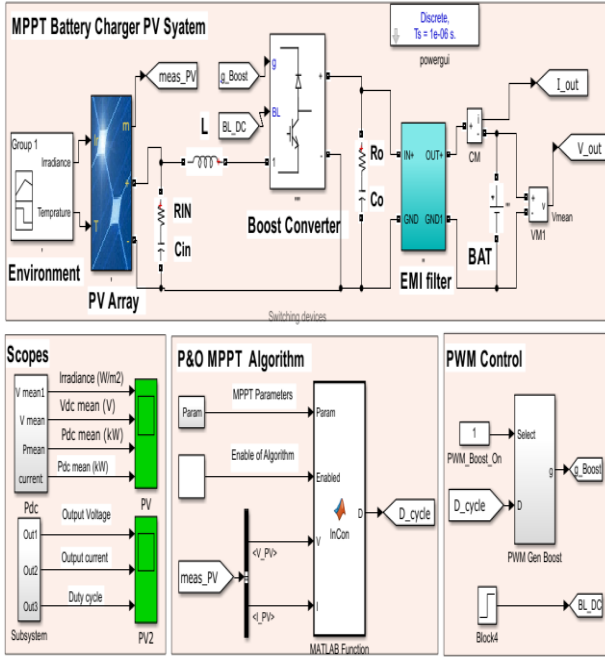


Fig. 5. Simulated PV system components and arrangement

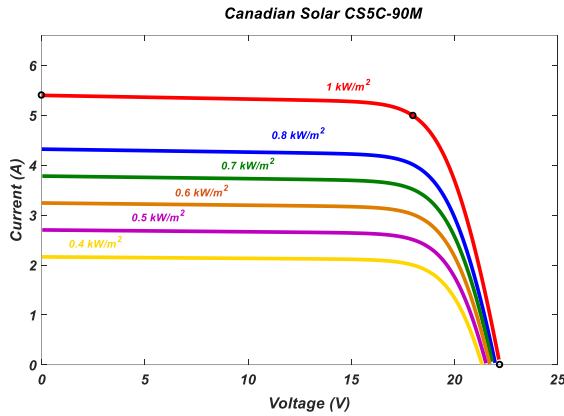


Fig. 6. I-V curves CANADIAN CS5C-90 panel

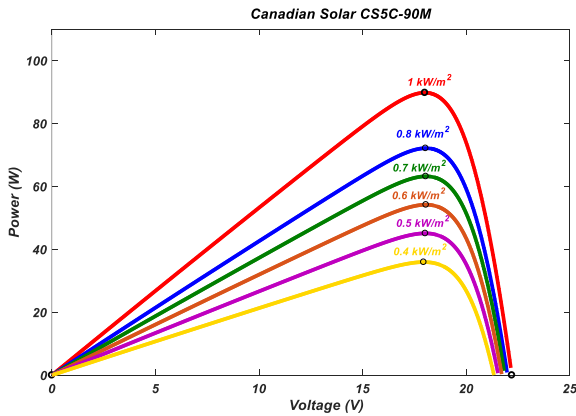


Fig. 7. P-V curves CANADIAN CS5C-90 panel

Other parameters are designed as in the following process.

Maximum Duty cycle of boost converter is calculates as in (5).

$$D_{max} = \frac{1 - 18}{24} = 0.25$$

The inductance of boost converter is calculated for required input ripple of current ΔI_L . Input ripple is taken as 20% of input current, that $\Delta I_L = 0.2 * 4.99 = 0.998$. The inductance is calculated as in (8).

$$L = \frac{18 * (24 - 18)}{0.998 * 50 * 10^3 * 24} = 90.2 * 10^{-6} H$$

The minimum output capacitor is calculated for required ripple of voltage ΔV_o . Output ripple is taken as 2% of output voltage, that $\Delta V_o = 0.02 * 24 = 0.48$. The conductance is calculated as in (10) and (11):

$$C_{min} = \frac{4 * 0.25}{50 * 10^3 * 0.48} = 42 * 10^{-6} F$$

$$ESR \leq \frac{1.2}{\left(4.99 + \frac{0.998}{2}\right)} = 218.6 * 10^{-3} ohm$$

The specification of boost converter is listed in Table 3. The output capacitor is chosen to be 68 μF and ESR is 200mH. Input capacitor is chosen as 330 μF with ESR of 38mH based on ΔV_{in} of 2%.

24V Battery bank (12V, 20AH, C/5) is used in the simulation. As can be shown in Fig. 5, constant voltage source is used to model the performance of battery ideally. This battery is charged by current that is supplied by MPPT system. This charging current is filtered through low pass filter.

TABLE 1. SPECIFICATION OF PV PANEL

Parameter	Value
STC (standard test conditions)	CS5C-90M
Nominal Maximum Power (Pmax)	90 W
Optimum Operating Voltage (Vmp)	18.0 V
Optimum Operating Current (Imp)	4.99 A
Open Circuit Voltage (Voc)	22.3 V
Short Circuit Current (Isc)	5.34 A

TABLE 2. SPECIFICATION OF DESIGN OF PV SYSTEM

Parameter	Value
Maximum output voltage V_{out}	24 V
Maximum Output Current I_{out}	4 A
Range of Input voltage V_{in}	22.1- 17.5 V
Switching Frequency of the system	50 KHz

TABLE 3. SPECIFICATION OF BOOST CONVERTER

Components	Value	Remark
Switching Device	IGBT	Chosen Ideally
Diode	Schottky	Chosen Ideally
Inductance	90.2 μ H	Equation (8)
Output Capacitor	68 μ F	ESR=200 mohm
Input Capacitor	330 μ F	ESR=38 mohm

5. Simulation Operation and Result

The simulation is run for different irradiance levels to simulate the real solar irradiation through a sunny day. The variation of temperature through a day could be taken constant approximately; because the decreasing of open circuit voltage of PV array is associated with increasing of short circuit current of PV array. Generally, there are many cases of environmental condition that represent different levels of irradiance through sunny day. In this simulation, two cases of environmental condition are taken under consideration which represent the most common conditions of environment. These two cases are slow changing environmental condition and fast changing environmental condition which are explained in the following points:

- Slow changing environment (SCE): Under this environmental condition, the level of irradiance changes slowly through the simulation periods to simulate the slow changing through normal day as shown in Fig. 8 which represents irradiance Levels of (600, 800, 1000, 700, 500) kw/m^2 respectively. In addition, the transition between irradiance levels is represented by ramp changing.

- Fast changing environment (FCE): Under this environmental condition, the level of irradiance changes rapidly through the simulation periods to simulate the rapid changing through normal day as shown in Fig. 9 which represents irradiance Levels of (600, 1000, 500) kw/m^2 respectively. In addition, the transition between irradiance levels is represented by ramp changing

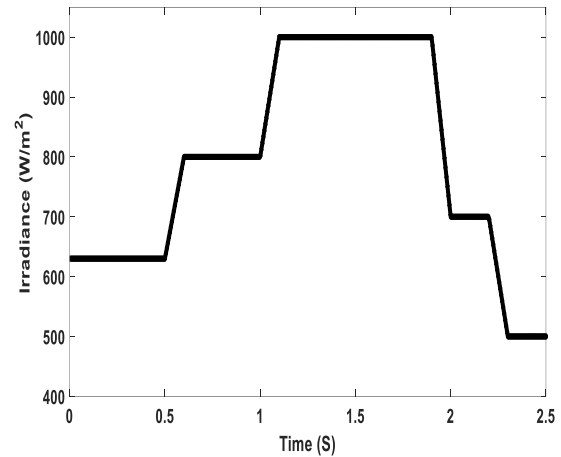


Fig. 8. Simulated Irradiance Levels Waveform under SEC

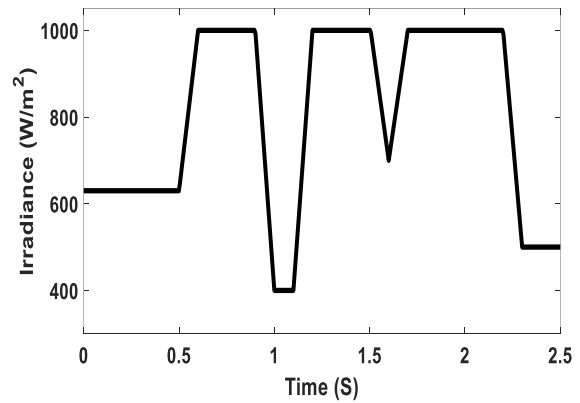


Fig. 9. Simulated Irradiance Levels Waveform under FEC

The effective operation of designed MPPT system under these different cases of environmental condition can be evaluated by analyzing carefully the performance of the system. There are many parameters that determine the performance of system. In this paper, three parameters are investigated which affect the performance of the system hardly. These parameters are tracking efficiency of MPPT system, conversion efficiency of MPPT system, and response time of MPPT system. These parameters are explained in details in following sections.

5.1 Tracking Efficiency of MPPT System

The tracking efficiency of MPPT system represents the capability of designed system on tracking MPP of PV panel under different conditions. The tracking efficiency of the designed MPPT system can be investigated through simulation results that are shown in Fig. 10 - 12 which represents voltage, current, and power of PV panel under SEC of environment respectively.

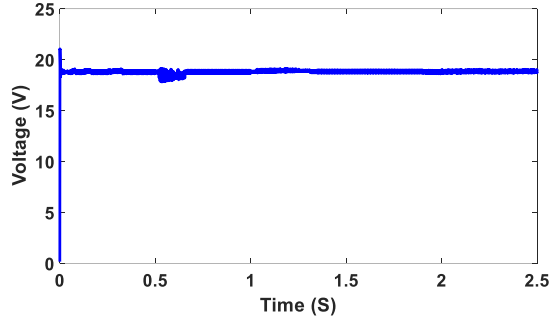


Fig. 10. Output simulation of PV voltage under SEC

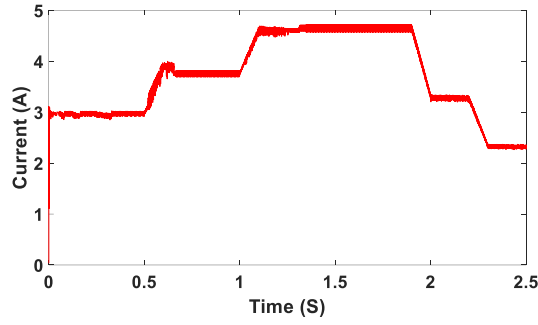


Fig. 11. Output simulation of PV current under SEC

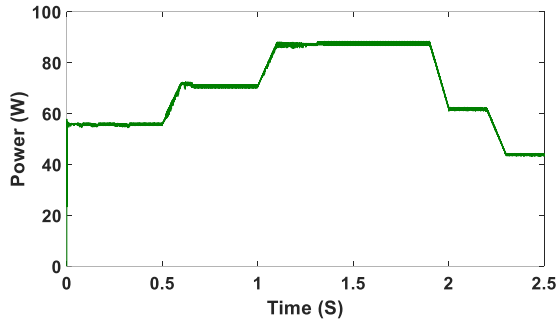


Fig. 12. Output simulation of PV power under SEC

In addition, tracking efficiency can be investigated through simulation results that are shown in Fig. 13 - 15 which represents voltage, current, and power of PV panel under FEC of environment respectively.

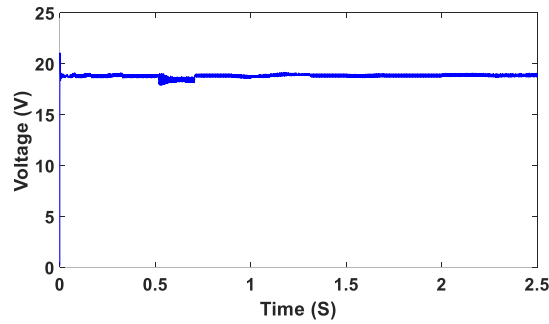


Fig. 13. Output simulation of PV voltage under FEC

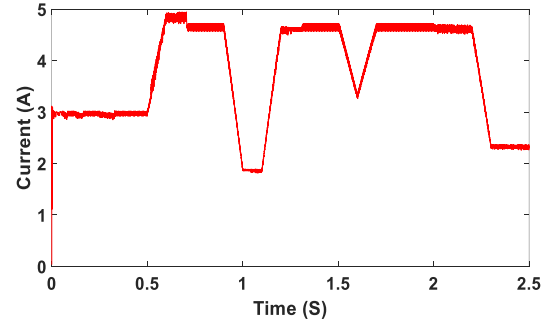


Fig. 14. Output simulation of PV current under FEC

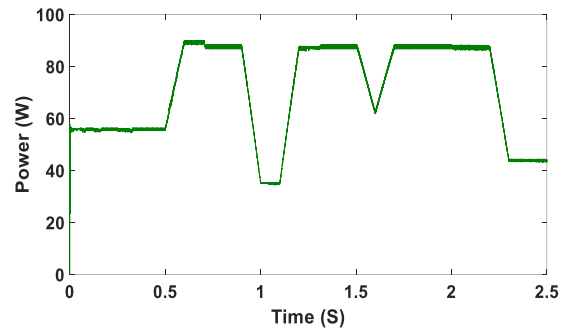


Fig. 15. Output simulation of PV power under FEC

The tracking efficiency of designed MPPT system under different level of irradiance can be computed numerically as shown in Table 4 and Table 5 for slow and fast changing conditions respectively.

In these table, the tracking efficiency of MPPT (Eff.) system at certain level of irradiance can be calculated taking the ratio between proposed maximum power ($P_{PV, \max}$) and averaged tracked maximum power ($P_{PV2, \max}$) by designed MPPT system.

$P_{PV, \max}$ can be obtained from P-V curve of PV panel at certain level of irradiance as shown in Fig. 7, whereas, $P_{PV2, \max}$ can be calculated from PV panel voltage ($V_{PV, av}$) and current ($I_{PV, av}$) that are averaged over the period of simulation.

TABLE 4. TRACKING EFFICIENCY OF DESIGNED SYSTEM UNDER SCE

IRRADIANCE W/M ²	P_{PV} (W) FIG.7	$V_{PV, AV}$ (V) FIG. 10	$I_{PV, AV}$ (A) FIG.11	$P_{PV1, AV}$ (W) FIG.12	EFF. %
1000	89.82	18.88	4.635	87.53	97.45
800	72.18	18.74	3.801	71.24	98.70
700	63.23	18.70	3.319	62.06	98.15
600	54.2	18.73	2.837	53.14	98.04
500	45.11	18.80	2.343	44.05	97.65

TABLE 5. TRACKING EFFICIENCY OF DESIGNED SYSTEM UNDER FCE

IRRADIANCE W/M ²	P _{PV} (W) FIG.7	V _{PV,AV} (V) FIG. 13	I _{PV,AV} (A) FIG.14	P _{PV2,AV} (W) FIG.15	EFF. %
1000	89.82	18.82	46.44	87.42	97.33
600	54.2	18.68	2.841	53.06	97.9
500	45.11	18.81	2.335	43.92	97.36
400	35.96	18.76	1.863	34.94	97.16

Depending on Table 4 and 5, tracking efficiency curve of designed MPPT system in term of solar irradiance level is constructed as shown in Fig. 16 and 17 under SCE and FCE respectively. As shown, average efficiency is 98% and 97.55% under SEC and FEC respectively.

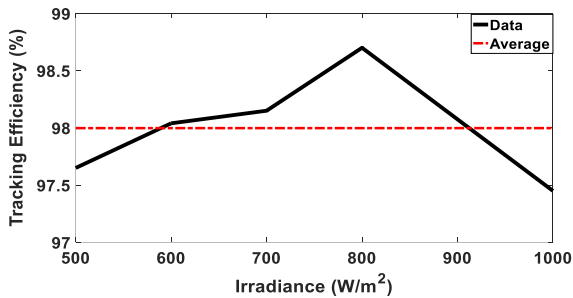


Fig. 16. Tracking efficiency curve in term of solar irradiance level under SCE

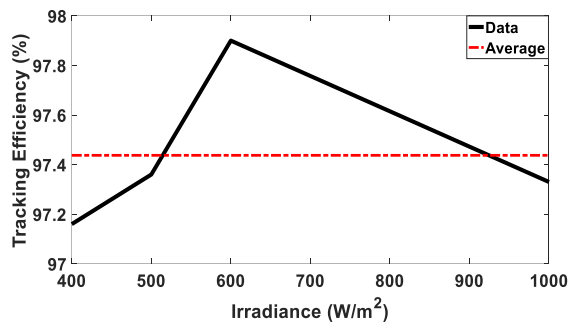


Fig. 17. Tracking efficiency curve in term of solar irradiance level under FCE

5.2 Conversion Efficiency of MPPT System

The conversion efficiency of MPPT system represents the amount of maximum power, which is extracted by MPPT system, which is available at the load (or battery) side of PV system. This efficiency is affected by the losses of MPPT system, which can be resulted from losses of boost converter.

The conversion efficiency of the designed MPPT system can be investigated through simulation results that are shown in Fig. 18 and 19 which represents current, and power of PV panel under SEC of environment respectively.

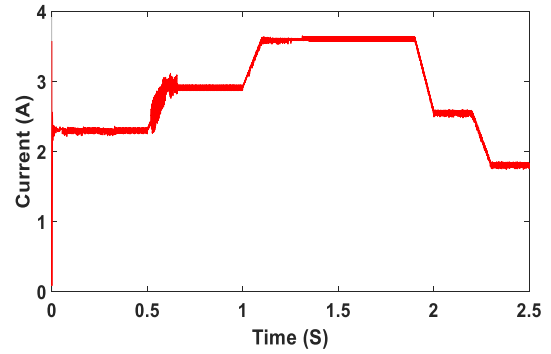


Fig. 18. Output Simulation of Battery Current under SCE

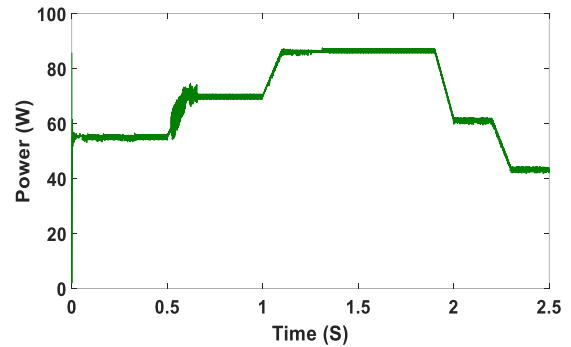


Fig. 19. Output Simulation of Battery Power under SCE

In addition, conversion efficiency can be investigated through simulation results that are shown in Fig. 20 and 21 which represents voltage, current, and power of PV panel under FEC of environment respectively.

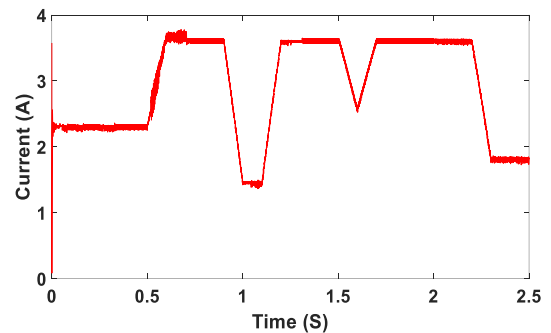


Fig. 20. Output Simulation of Battery Current under FCE

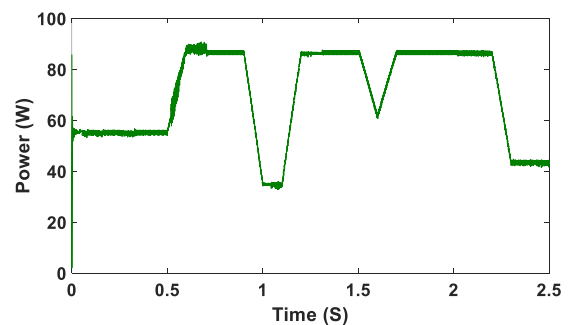


Fig. 21 Output Simulation of Battery Power under FCE

The conversion efficiency of designed system under different level of irradiance can be computed numerically as shown in in Table 6 and Table 7 for slow and fast changing conditions respectively.

TABLE 6. CONVERSION EFFICIENCY OF DESIGNED SYSTEM UNDER SCE

IRRADIANCE W/M ²	P _{PV1,av} (W) FIG.12	V _{BAT,av} (V)	I _{BAT,av} (A) FIG.18	P _{BAT,av} (W) FIG.19	EFF. %
1000	87.53	24	3.604	86.5	98.82
800	71.24	24	2.931	70.35	98.75
700	62.06	24	2.55	61.20	98.61
600	53.14	24	2.188	52.52	98.83
500	44.05	24	1.751	43.00	97.6

TABLE 7. CONVERSION EFFICIENCY OF DESIGNED SYSTEM UNDER FCE

IRRADIANCE W/M ²	P _{PV2,av} (W) FIG.15	V _{BAT,av} (V)	I _{BAT,av} (A) FIG.20	P _{BAT,av} (W) FIG.21	EFF. %
1000	87.42	24	3.6	86.50	98.91
600	53.06	24	2.17	52.19	98.36
500	43.92	24	1.79	42.98	97.86
400	34.94	24	1.42	34.18	97.82

In these table, the conversion efficiency (Eff.) of MPPT system at certain level of irradiance can be calculated by taking the ratio between maximum extracted power $P_{PV1, \max}$ and $P_{PV2, \max}$ at different level of irradiance, and supplied power to battery $P_{BAT,av}$ which can be calculated from battery voltage ($V_{BAT,av}$) and current ($I_{BAT,av}$).

Depending on Table 6 and 7, conversion efficiency curve of designed MPPT system in term of solar irradiance level is constructed as shown in Fig. 22 and 23 under SCE and FCE respectively. As shown, average efficiency is 98.52% and 98.24% under SEC and FEC respectively.

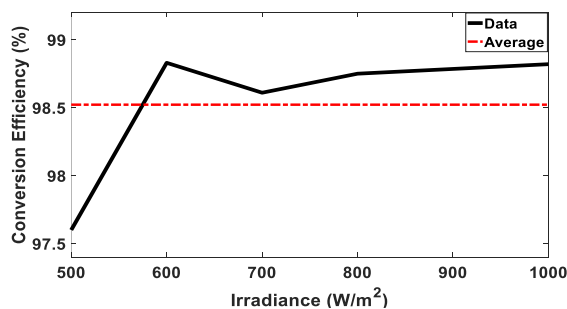


Fig. 22. Conversion efficiency curve in term of solar irradiance level under SCE

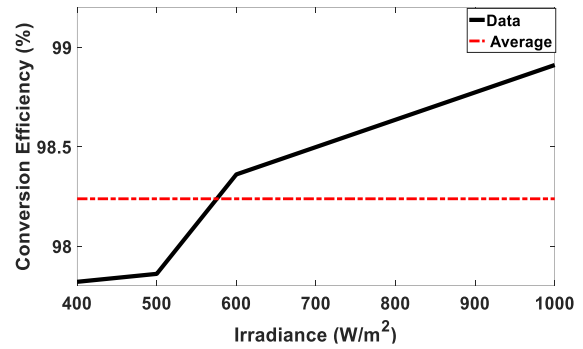


Fig. 23. Conversion efficiency curve in term of solar irradiance level under FCE

5.3 Response Time of MPPT System

In this research, response time of MPPT system is defined as the time required by PV power to settle within the tolerance interval of maximum power point of PV panel when a change of irradiance level is occurred.

Therefore, response time of designed MPPT system is computed numerically as shown in Table 8 and Table 9 for slow and fast changing conditions respectively. In these tables, T_{res} represents the total time required by MPPT to track the changing of irradiance level until and bring the PV power into specific tolerance of MPP of PV panel, T_{cha} represents the time of changing of irradiance between two levels, and ΔT represent the response time of designed MPPT system.

The values of T_{rs} and T_{cha} parameters are determined from transition periods of Fig. 12 and 15 for SCE and FCE respectively

TABLE 8. RESPONSE TIME UNDER SCE

Irradiance KW/m2	T _{res} (ms)	T _{cha} (ms)	ΔT (ms)
600-800	140	100	40
800-1000	142	100	42
1000-700	116	100	16
700-500	112	100	12

TABLE 9. RESPONSE TIME UNDER FCE

Irradiance KW/m2	T _{res} (ms)	T _{cha} (ms)	ΔT (ms)
600-1000	166	100	66
1000-400	145	100	45
400-1000	170	100	70
1000-700-1000	220	200	20
1000-500	130	100	30

As shown in Tables 8 and 9, the maximum ΔT time required to settle the ripples of power is in the range of 70ms in both cases of environmental condition. This delay is small compared with 2.5 s which is the selected time of simulation to represent the changing of environmental condition through a day.

6. Conclusion

The design of MPPT controlled boost converter has been presented. When PV system is used to charge battery, it crucial to use DC-DC converter as interface MPPT unit in order to achieve the matching between battery and PV system, and ensure the operating of PV panel in MPP. The InC algorithm has been used to control the duty cycle of converter directly through PWM operating in 50 kHz. The overall system has been simulated and validated in SIMULINK MATLAB. The high performance of the designed MPPT system has been proved under slow and fast changing environmental conditions. The high performance of this design could be shown through its ability to track the MPP of PV panel with efficiency of 98% and 97.55% for slow and fast condition respectively. In addition, the designed system can convert power to battery system with efficiency of 98.52% and 98.23% for slow and fast condition respectively. Furthermore, the designed system has been proved for its high response time. In this simulated system, the battery is represented by constant voltage ideally that does not affect the operation of MPPT system and efficiency of whole system. Practically, the parameter of battery, such as charging current, charging voltage, state of charge, temperature of battery, should be taken into account in designing MPPT system in order to ensure the operation of the system with high efficiency. In future work, the designed proposed in this system will be verified practically.

References

1. Mekhilef, S., Saidur, R., Safari, A.: *A review on solar energy use in industries*. In: Journal of Renewable and Sustainable Energy, Vol. 15, No. 4, 2011, p. 1777 – 1790.
2. Reddy, B.R.S., Jambholkar, P., Narayana, P.B., Reddy, K.S.: *MPPT algorithm implementation for solar photovoltaic module using microcontroller*. In: Proceedings of Annual IEEE India Conference (INDICON-2011), 2011, Hyderabad, India, p. 1-3
3. Shanta, K.K., Prema, V., Uma, K., Meena, P.: *Efficient MPPT for a stand-alone photovoltaic system*. In: Proceedings of International Conference on Renewable Energy and Sustainable Energy [ICRESE'13], 2013, Coimbatore, India, p. 213-220.
4. Subashini, M., Ramaswamy, M.: *A novel design of charge controller for a standalone solar photovoltaic system*. In: Proceedings of 3rd International Conference on Electrical Energy Systems (ICEES), 2016, Chennai, India, p. 237-243
5. Hussein, K.H., Muta, I., Hoshino, T., osakada, M.: *Maximum Power Point Tracking an Algorithm for Rapidly Changing Atmospheric Conditions*. In: IEE Proceedings of Generation, Transmission and Distribution, Vol. 142, No. 1, 1995, p. 59 – 64.
6. Mohammed, S.S., Devaraj, D.: *Simulation of incremental conductance MPPT based two phase interleaved boost converter using MATLAB SIMULINK*. In: Proceedings of IEEE International Conference on Electrical, Computer and Communication Technologies (ICECCT), 2015, Coimbatore, India, p. 1 – 6.
7. Anuradha, T., Sundari, PD., Padmanaban, S., Siano, P., Leonowicz, Z.: *Comparative analysis of common MPPT techniques for solar PV system with soft switched, interleaved isolated converter*. In: Proceedings of IEEE International Conference on Environment and Electrical Engineering and IEEE Industrial and Commercial Power Systems Europe (EEEIC / I&CPS Europe), 2017, Milan, Italy, p. 1 – 6
8. Zaghba, L., Borni, A., Bouchakour, A., Terki, N.: *Buck-boost converter system modelling and incremental inductance algorithm for photovoltaic system via photovoltaic cell*. In: Proceedings of Revue des Energies Renouvelables SIENR'14, 2012, Ghardaia, Algeria, p. 63-70.
9. Rashid, H.M.: *Power Electronics Handbook*, Academic Press, Canada, 2011.
10. Mohamed, H.M., Khattab, A., Mobarka, H.A., Morsy, G.A.: *Design, control and performance analysis of DC-DC boost converter for stand-alone PV system*. In: Proceedings of Eighteenth International Middle East Power Systems Conference (MEPCON), 2016, Cairo, Egypt, p. 101–106
11. Sahu, P., Verma, D., Nema, S.: *Physical design and modelling of boost converter for maximum power point tracking in solar PV systems*. In: Proceedings of International Conference on Electrical Power and Energy Systems (ICEPES), 2016, Bhopal, India, p. 14-16.
12. Lyden, S., Haque, M., Gargoom, A., Negnevitsky, M., Muoka, PI.: *Modelling and parameter estimation of photovoltaic cell*. In: Proceedings of 22nd Australasian Universities Power Engineering Conference (AUPEC), 2014, Bali, Indonesia, p. 63-70.